Published in final edited form as:
Biochemistry. 2011 May 3; 50(17): 3570–3577. doi:10.1021/bi200113y.

A second target of the antimalarial and antibacterial agent fosmidomycin revealed by cellular metabolic profiling†

Baichen Zhang[a], **Kristin M. Watts**[b], **Dana Hodge**[b], **Lisa M. Kemp**[b], **David A. Hunstad**[b,c], **Leslie M. Hicks**[a], and **Audrey R. Odom**[b,*]

[a]Proteomics & Mass Spectrometry Facility, Donald Danforth Plant Science Center, St. Louis, MO 63132

[b]Department of Pediatrics, Washington University School of Medicine, St. Louis, MO 63110

[c]Department of Molecular Microbiology, Washington University School of Medicine, St. Louis, MO 63110

Abstract

Antimicrobial drug resistance is an urgent problem in control and treatment of many of the world's most serious infections, including *Plasmodium falciparum* malaria, tuberculosis, and healthcare-associated infections with Gram-negative bacteria. Because the non-mevalonate pathway of isoprenoid biosynthesis is essential in eubacteria and *P. falciparum*, and this pathway is not present in humans, there is great interest in targeting the enzymes of non-mevalonate metabolism for antibacterial and antiparasitic drug development. Fosmidomycin is a broad-spectrum antimicrobial agent currently in clinical trials of combination therapies to treat malaria. In vitro, fosmidomycin is known to inhibit the deoxyxylulose phosphate reductoisomerase (DXR) enzyme of isoprenoid biosynthesis from multiple pathogenic organisms. To define the in vivo metabolic response to fosmidomycin, we developed a novel mass spectrometry method to quantitate six metabolites of non-mevalonate isoprenoid metabolism from complex biological samples. Using this technique, we validate that the biological effects of fosmidomycin are mediated through blockade of de novo isoprenoid biosynthesis in both *P. falciparum* malaria parasites and *E. coli* bacteria: in both organisms, metabolic profiling demonstrated a block in isoprenoid metabolism following fosmidomycin treatment, and growth inhibition due to fosmidomycin was rescued by media supplemented with isoprenoid metabolites. Isoprenoid metabolism proceeded through DXR even in the presence of fosmidomycin, but was inhibited at the level of the downstream enzyme, methylerythritol phosphate cytidyltransferase (IspD). Overexpression of IspD in *E. coli* conferred fosmidomycin resistance, and fosmidomycin was found to inhibit IspD in vitro. This work has validated fosmidomycin as a biological reagent to block non-mevalonate isoprenoid metabolism, and suggests a second in vivo target for fosmidomycin within isoprenoid biosynthesis, in two evolutionarily diverse pathogens.

Isoprenoids comprise a large, diverse group of intracellular metabolites with multiple cellular functions, including roles in membrane structure, cellular respiration, and cell signaling (1). Two distinct biosynthetic routes exist to produce isopentenyl diphosphate

†This work was supported by NIH K08 AI079010 and the Children's Discovery Institute of St. Louis, MO. A.R.O. is a Scholar of the Child Health Research Center of Excellence in Developmental Biology at Washington University (K12-HD01487). Funding for the 4000 QTRAP mass spectrometer was provided through an NSF-MRI grant (DBI-0521250).

*To whom correspondence should be addressed: 660 S. Euclid Ave., Campus Box 8208, St. Louis, MO 63110. Phone: (314)-747-2370. Fax: (314)-286-2895. odom_a@kids.wustl.edu.

Supporting Information Available. Supplementary methods and figures (Fig. S1, S2, S3, S4, S5, and S6) are provided. This material is available free of charge via the Internet at http://pubs.acs.org.

(IPP)[1] and dimethylallyl diphosphate (DMAPP), the basic isoprenoid building blocks. Mammals, including humans, exclusively utilize the classic metabolic route through mevalonate. In contrast, eubacteria, cyanobacteria, and plant chloroplasts use an alternative route that produces the key intermediate 1-D-deoxyxylulose 5-phosphate (DOXP) from pyruvate (Fig. 1) (2). In bacteria that use this pathway, including *Escherichia coli* and *Mycobacterium tuberculosis*, genetic studies have demonstrated that non-mevalonate isoprenoid biosynthesis is essential (3, 4).

The malaria parasite *Plasmodium falciparum* annually kills nearly one million people, primarily young children (5, 6). There is widespread resistance to older antimalarial drugs, such as chloroquine, and emerging resistance to new artemisinin-based therapies (7, 8). *P. falciparum* also utilizes non-mevalonate isoprenoid biosynthesis, which is essential to the parasite (9–11). Novel non-mevalonate pathway inhibitors therefore hold great promise as antimicrobial agents with broad activity against major human pathogens, including *P. falciparum*, *M. tuberculosis*, and enterobacteria, in which global drug resistance has created an urgent need.

The first dedicated step of non-mevalonate isoprenoid biosynthesis is accomplished by the bifunctional enzyme deoxyxylulose 5-phosphate reductoisomerase (DXR, EC 1.1.1.267). DXR is competitively inhibited in vitro by the antibiotic fosmidomycin, which also inhibits the DXR-like (DRL) enzyme from *Bacillus abortus* (12, 13). Fosmidomycin has shown clinical promise as an antimalarial agent: it inhibits recombinant *P. falciparum* DXR, kills the malaria parasite, and is currently in Phase II clinical trials in combination therapy with clindamycin for malaria (10, 14).

Since any small molecule inhibitor may have unintended “off-target” cellular effects, biochemical validation of small molecule inhibitors in vivo is an important step in drug development. This was highlighted recently by the discovery that the in vitro target (enoyl-ACP reductase) of the antimalarial triclosan is in fact dispensable for blood-stage parasite development (15). Since fosmidomycin inhibits DXR in vitro, it is predicted to reduce intracellular concentrations of the DXR product, methylerythritol phosphate (MEP). However, three studies have examined fosmidomycin-treated *P. falciparum* parasites by metabolic labeling and found few changes in any non-mevalonate metabolite following fosmidomycin treatment (9, 16, 17). Notably, none of these studies observed a substantial decrease in MEP levels in fosmidomycin-treated trophozoite stage parasites, the most metabolically active intraerythrocytic stage of malaria parasite growth. Although recombinant DXR from *E. coli* and *P. falciparum* have excellent concordance in sensitivities to a variety of fosmidomycin analogs (18), several fosmidomycin derivatives with poor activity against *E. coli* DXR have augmented antimalarial properties (19, 20). These studies raise the possibility that the antimicrobial effects of fosmidomycin might not be exerted exclusively through DXR inhibition.

Flux through the non-mevalonate pathway has previously been described using metabolic labeling with [^{14}C]-labeled precursors and HPLC analysis (9, 21). Here, we describe a novel mass spectrometry (LC-MS/MS) technique to simultaneously and quantitatively detect six metabolites of the non-mevalonate pathway in biologic samples, eliminating the need for radiochemical synthesis. Using this technique in two evolutionarily diverse microbes (*E. coli* and *P. falciparum*), we confirm the biological effects of fosmidomycin are due to inhibition

[1]Abbreviations: IPP, isopentenyl diphosphate; DMAPP, dimethylallyl diphosphate; DOXP, 1-D-deoxyxylulose 5-phosphate; DXR, deoxyxylulose phosphate reductoisomerase; MEP, methylerythritol phosphate; MRM, multiple reaction monitoring; LC-MS, liquid chromatography-mass spectrometry; ME, methylerythritol; CDP-ME, cytidine diphosphate methylerythritol; CDP-MEP, cytidine diphosphate methylerythritol phosphate; cMEPP, cyclic methylerythritol diphosphate; LC, liquid chromatography; IPTG, isopropyl β-D-1-thiogalactopyranoside; TMS, trimethylsyl; PBS, phosphate buffered saline; GG-ol, geranylgeraniol.

of isoprenoid metabolism. Our results support a model in which fosmidomycin directly inhibits its known target, DXR, and indirectly acts upon cells to inhibit a second target, the downstream enzyme methylerythritol phosphate cytidyltransferase (IspD).

Experimental procedures

LC-MS/MS analysis

The 4000 QTRAP LC-MS/MS system (Applied Biosystems) was used in multiple reaction monitoring (MRM) mode using negative ionization. Detailed instrument configuration was as previously described (22), and compound-dependent parameters for isoprenoid precursors (Echelon, Salt Lake City, UT) are provided in Table 1. LC separation prior to MRM detection was achieved by ion-pair reverse-phase chromatography as described (23), with 10 mM tributylammonium acetate (pH 5.1–5.5) used as ion pair reagent and with the following modifications: 1) HPLC column: RP-hydro 100×2.0 mm 2.5 μM (Phenomenex, CA); 2) Flow rate: 0.19 ml/min; 3) Binary LC gradient: 0–5 min 10% solvent B, 20 min 60% B, 21 min 100% B, 26.1 min 100% B, 27 min 10% B, and column equilibration for 8 min; and 4) Autosampler injection volume: 20 μL. Accurate mass measurements were obtained using LC-MS on an Agilent 6520 ESI-Q-TOF mass spectrometer. GC-MS data of TMS derivatives from dried LC fractions were acquired on an Agilent 5976C instrument equipped with an HP-5 column (Agilent, Santa Clara, CA).

Plasmodium falciparum culture

P. falciparum strain 3D7, provided by Daniel Goldberg (Washington University, St. Louis, MO), was cultured in vitro in human erythrocytes as described (24), with modifications: 5% O_2/5% CO_2/90% N_2 atmosphere in RPMI 1640 (Sigma) media, supplemented with 27 mM sodium bicarbonate, 11 mM glucose, 5 mM HEPES, 1 mM sodium pyruvate, 0.37 mM hypoxanthine, 0.01 mM thymidine, 0.25 mg/ml gentamicin, and 0.5% Albumax (Gibco). Cultures were treated twice with 5% (w/v) D-sorbitol solution during ring-stage growth to produce a greater than 90% synchronized culture. Giemsa-stained smears were used to follow growth.

Sample preparation for mass spectrometry analysis

P. falciparum cultures were grown in 200 mL volumes at 4% hematocrit until 10% parasitemia. For fosmidomycin-treated samples, 5 μM fosmidomycin (Invitrogen) was added to ring-stage cultures at t=0, and 20 mL samples of parasite culture were removed at t=0 and t=10 h. Infected erythrocytes were lysed with 0.5% saponin, and parasite-containing pellets were washed with phosphate-buffered saline (PBS), dried, and stored at −80°C until extraction. For *E. coli* cultures, single colonies of strain MG1655 were grown to saturation at 37°C with shaking in 3 mL Luria-Bertani (LB) broth. Saturated cultures were subcultured 1:100 into 25 mL LB. At log phase (OD_{600} of 0.6, t=0), cultures were treated with 2.5 μM fosmidomycin. At each timepoint, 5 mL of culture was harvested by centrifugation, washed with PBS, and stored at −80°C. Samples were extracted by addition of 250–500 μL ice-cold extraction solvent [chloroform, methanol, and acetonitrile (2:1:1 v/v/v)] and two liquid nitrogen-cooled 3.2 mm stainless steel beads, followed by homogenization in the TissueLyser II (Qiagen, Valencia, CA) at 15 Hz for 10 min in a cold sample rack. Ice-cold water (2 vol) was added, and samples were homogenized for another 10 min at 15 Hz. After centrifugation (1.2×10^4 rcf, 4°C, 4 min), the polar upper phase was aspirated and lyophilized. Dried samples were dissolved in ice-cold water and analyzed by LC-MS/MS.

P. falciparum growth inhibition assay

Asynchronous 3D7 *P. falciparum* cultures were diluted to 1% total parasitemia in 2% hematocrit and grown in 96-well flat-bottomed opaque plates (Corning Incorporated, Corning, NY) at 100 μL/well. Geranylgeraniol (Sigma, 1:1 cis:trans, >85% purity) was solubilized in ethanol and then diluted in malaria media. 2-C-methyl-D-erythritol (ME) (Echelon, Salt Lake City, UT, >99% purity) was diluted directly into malaria growth medium. In rescue experiments, dilutions of metabolites were added to cultures also treated with 1.5 μM fosmidomycin (Invitrogen). After three days, parasitemia was quantified using the DNA fluorophore PicoGreen (Molecular Probes), as described (25). Fluorescence (proportional to DNA content) was quantified on a Synergy 2 Multi-Mode Microplate Reader (BioTek Inc., Winooski, VT) at 485/20 nm excitation and 528/20 nm emission, and data were analyzed using the manufacturer's Gen5 software.

E. coli growth inhibition assay

Overnight cultures of *E. coli* strain MG1655 were diluted 1:100 into fresh LB medium and grown to an OD_{600}=1. Cultures were diluted to 10^5 cfu/mL in 100 μL/well of a 96-well plate, with indicated amounts of fosmidomycin and rescue compounds. Bacteria were grown in the BioTek Synergy 2 microplate reader at 37°C, 250 rpm, with serial OD_{600} measurements. Expression vectors (described in supplemental methods) were maintained in transformed strains by 100 μg/mL ampicillin, with or without addition of 0.1 mM IPTG to further induce protein expression. GraphPad Prism Software was used to calculate inhibitory constants (IC_{50} values).

Hazardous procedures

P. falciparum is classified as a Biosafety Level 2 pathogen, and was maintained in an appropriate facility using established safety protocols.

Results

Quantitative detection of non-mevalonate isoprenoid biosynthesis metabolites by LC-MS/MS

In order to analyze non-mevalonate isoprenoid biosynthesis, we developed a method to simultaneously measure the first five pathway metabolites: DOXP, MEP, cytidine diphosphate methylerythritol (CDPME), cytidine diphosphate methylerythritol phosphate (CDP-MEP), and cyclic methylerythritol diphosphate (cMEPP) (Fig. 1). This sensitive and specific LC-MS/MS method utilizes multiple reaction monitoring (MRM) to quantify compounds from complex sample matrices such as total parasite and bacterial extracts. Since CDP-MEP is not commercially available, we predicted MRM transitions according to CDP-ME MS/MS spectra and confirmed these predictions using enzymatically synthesized CDP-MEP (Fig. S1). Commercially available DOXP, MEP, CDP-ME, and cMEPP (>99% purity) were used as standards to determine liquid chromatography (LC) and mass spectrometry (MS) conditions (Table 1) for optimal resolution and detection of each compound (Fig. S2).

LC-MS/MS method detects isoprenoid precursors without significant ion suppression

Quantitative MS detection in biological samples can be hindered by ion suppression, in which complex metabolites in extracts interfere with the sensitivity and accuracy of compound measurement. Ion suppression was routinely observed in the initial method development with a standard C18 reverse-phase LC column operating in ion pair mode. Although separation of isoprenoid precursor standards was achieved with several reverse phase columns, matrix ion suppression was avoided only through use of ion pair

chromatography using an RP-Hydro C18 column. Commercial standards were analyzed by LC-MS/MS, before and after spiking with malaria parasite extracts, to confirm the absence of ion suppression (Fig. 2). This method sensitively detected non-mevalonate metabolites in biological samples (Fig. S3).

Detection of the DXR enzymatic intermediate, 2-C-methylerythrose 4-phosphate

The two-step reductoisomerase reaction of DXR has been described to proceed via isomerization of DOXP to a reaction intermediate, 2-C-methylerythrose 4-phosphate, which is then reduced to MEP (26, 27). Pilot LC-MS/MS analyses in both malaria parasites and *E. coli* bacteria revealed a novel compound that did not correspond to commercial standards, nor to predicted CDP-MEP fragments. We analyzed this compound further to establish its probable identity as 2-C-methylerythrose 4-phosphate.

Via LC-MS/MS, this metabolite was characterized by an MRM transition corresponding to one of the DOXP transitions (213/79), but with a unique retention time eluting before MEP, suggesting that it was structurally related to, but distinct from, DOXP. Accurate mass analysis of this unknown peak revealed an *m/z* of 213.01677 and a predicted and calculated empirical formula of $C_5H_{11}O_7P$ (Calc. 213.01696; −0.9 ppm difference). The diagnostic 139 ion of DOXP is formed after cleaving the acetol moiety (empirical formula, $C_2H_4O_5P$). Fragmentation of the unknown metabolite resulted in product ions at *m/z* 79 and 97, but the 139 ion was missing (Fig. S4). In addition, there was also no water loss observed during fragmentation. Both these findings indicated that the unknown 214 Da metabolite either lacks a hydroxyl group and/or has a unique hydroxyl arrangement not shared by DOXP. The mass of DOXP is identical to the mass of both the isomerized DXR reaction intermediate, 2-C-methylerythrose 4-phosphate, and the unknown compound (i.e., 214.02424 Da). Furthermore, the fragmentation we observed was consistent with the structure of 2-C-methylerythrose 4-phosphate; this compound does not contain a hydrogen in its beta-carbon position, which would both inhibit the formation of the characteristic 139 ion (seen in DOXP) and reduce water loss.

To characterize the 214 Da metabolite further, we chromatographically purified this compound and performed gas chromatography-mass spectrometry (GC-MS). Ion-pair chromatography fractions containing the 214 Da species and DOXP were collected separately, derivatized by N-methyl-N-trifluoroacetamide (MSTFA), and analyzed by GC-MS (Fig. S4). The dominant trimethylsyl (TMS) derivative peak containing a phosphate group was compared with TMS derivatives of the DOXP fraction, used as a control. No known spectra corresponding to this compound were identified in the NIST 08 GC-MS database. The dominant peak containing a phosphate group shares similarity with the control fraction of DOXP, confirming that they are closely structurally related. Our MS and MS/MS data are therefore consistent with detection of the predicted DXR reaction intermediate, 2-C-methylerythrose 4-phosphate. Absolute confirmation of the predicted structural identity of the 214 Da species as 2-C-methylerythrose 4-phosphate will require chemical synthesis or NMR analysis of purified compound, both of which are technically challenging due to the labile nature of this aldehyde.

Fosmidomycin treatment blocks isoprenoid metabolism at the level of methylerythritol phosphate cytidyltransferase (IspD)

The developed LC-MS/MS method was utilized to detect metabolic changes in the non-mevalonate pathway in fosmidomycin-treated *P. falciparum* malaria parasites. Synchronized *P. falciparum* parasites were analyzed as ring stage parasites (t=0) and allowed to continue development to the highly metabolically active trophozoite stage (t=10h) with and without fosmidomycin. Five of the six non-mevalonate pathway metabolites could be quantified

(DOXP, 2-C-methylerythrose 4-phosphate, MEP, CDP-ME, and cMEPP; representative MRM trace, Fig. S3). CDP-MEP was detectable in malaria parasites, but was below the level of accurate quantitation. During trophozoite development, cellular concentrations of all detected metabolites more than doubled, which is consistent with known increases in metabolic activity and in transcript levels of apicoplast-targeted genes (including all isoprenoid metabolic enzymes) during this developmental stage (28). Striking metabolic changes were observed in fosmidomycin-treated parasites compared to controls. Fosmidomycin-treated parasites demonstrated a substantial reduction in the concentrations of the most distal isoprenoid metabolites (CDP-ME and cMEPP) (Table 2). Levels of the DXR substrate, DOXP, rose compared to untreated cells. Surprisingly, however, levels of the two products of the DXR enzyme (the intermediate, 2-C-methylerythrose 4-phosphate, and final product, MEP) did not decrease after fosmidomycin treatment as expected, but instead increased compared to the control. These results suggest that fosmidomycin does not exclusively block isoprenoid biosynthesis through inhibition of DXR enzyme. Instead, since MEP levels rise and CDP-ME levels fall, fosmidomycin treatment might also inhibit the downstream methylerythritol phosphate cytidyltransferase enzyme (IspD) that converts MEP to CDP-ME.

Since several aspects of metabolism in *P. falciparum* parasites are unique, we analyzed the metabolic response to fosmidomycin in the model Gram-negative bacterium, *E. coli*. *E. coli* cultures in logarithmic growth were treated with fosmidomycin, and samples were harvested for LC-MS/MS analysis. Serial samples from the same culture were compared before and after fosmidomycin treatment. Metabolic changes observed in fosmidomycin-treated *E. coli* bacteria were similar to those measured in *P. falciparum* parasites. All six non-mevalonate pathway metabolites were detected and quantified in *E. coli* (representative MRM trace, Fig. S3). Following fosmidomycin treatment, levels of the most distal isoprenoid metabolites (CDP-ME, CDP-MEP, and cMEPP) fell below the level of detection within one hour (less than 1% of pretreatment levels, using the calculated lower limits of detection for each compound) (Table 3). DOXP levels rose signficantly (over 25-fold) following fosmidomycin treatment. As in malaria parasites, the pattern of isoprenoid blockade was not consistent with competitive inhibition of DXR, since the cellular concentration of the DXR reaction intermediate 2-C-methylerythrose 4-phosphate (undetectable prior to fosmidomycin treatment) rose dramatically and levels of the final DXR product (MEP) were stable following fosmidomycin treatment.

Downstream isoprenoids rescue fosmidomycin-treated malaria and *E. coli*

Alcohol forms of nonmevalonate pathway intermediates are predicted to permeate cells and be phosphorylated by cellular kinases to enter the non-mevalonate isoprenoid biosynthesis pathway. This has been clearly demonstrated in *E. coli*, since media supplementation with the alcohol form (methylerythritol, ME) of the DXR product (MEP) rescues the lethality of a DXR null mutation (3). Although 0.1 mM ME (sufficent to rescue a DXR null mutant) improved the growth of fosmidomycin-treated *E. coli* cells, more substantial growth improvement was noted only at high doses of ME (1 mM) (Fig. 3A). In contrast, the alcohol form of the downstream isoprenoid geranylgeraniol (GG-ol, alcohol of geranylgeranyl diphosphate) almost fully rescued fosmidomycin-treated *E. coli* at 0.1 mM. Higher concentrations of GG-ol inhibited *E. coli* growth, and therefore complete rescue by GG-ol was not observed. These data strongly support that bacterial growth inhibition by fosmidomycin is mediated through both DXR inhibition and also through blockade of isoprenoid metabolism downstream of DXR.

For *P. falciparum*, there was no improvement in fosmidomycin sensitivity with ME supplementation (to 1 mM) (Fig. 3B). This may reflect fosmidomycin inhibition of enzymes downstream of DXR, or poor ME penetration to the apicoplast organelle of the malaria

parasite (where isoprenoid biosynthesis takes place), which is surrounded by an additional four membrane bilayers (29). Supplementation with the downstream isoprenol GG-ol fully rescued the antimalarial effects of fosmidomycin.

IspD overexpression confers resistance to fosmidomycin

Overexpression of enzymatic targets typically decreases cellular sensitivity to inhibitors, since more inhibitor is required to block all enzymatic function. We transformed *E. coli* with either an empty vector or vectors that overexpressed either *E. coli* DXR or IspD protein. The half-maximal inhibitory concentration (IC_{50}) of fosmidomycin was determined for each strain at 10h of growth (Fig. 4). Overexpression of the known target protein DXR increased the IC_{50} more than 6-fold (from 0.118 +/− 0.003 μM to 0.794 +/− 0.093 μM; p = 0.018). Overexpression of IspD more than doubled the IC_{50} of fosmidomycin in *E. coli* (to 0.239 +/− 0.013 μM; p = 0.013), suggesting that both proteins represent in vivo targets.

Fosmidomycin inhibits purified IspD enzyme

In vivo, fosmidomycin may inhibit IspD directly, or may cause other changes within the cell that reduce IspD activity. We therefore evaluated the ability of fosmidomycin to inhibit the activity of purified recombinant IspD directly, using a linked enzymatic assay to detect release of pyrophosphate (Fig. S5). Fosmidomycin directly inhibits Ec-IspD at high concentrations (Fig. 5), while purified Ec-DXR was readily inhibited by fosmidomycin.

Discussion

The phosphonic acid antibiotic fosmidomycin inhibits the deoxyxylulose 5-phosphate reductoisomerase (DXR) enzyme of non-mevalonate isoprenoid biosynthesis from multiple organisms in vitro (10, 27, 30). The broad antibacterial and antimalarial activities of fosmidomycin have fueled interest in development of additional drugs that target the non-mevalonate pathway of isoprenoid biosynthesis. As novel inhibitors of these enzymes are developed, methods to confirm their intracellular metabolic effects will be required. This study describes a novel LC-MS/MS method that quantitatively detects non-mevalonate metabolites from complex biological systems. We have used this method to describe the temporal changes in non-mevalonate pathway metabolism in two evolutionarily distinct human pathogens, *E. coli* and the malaria parasite *P. falciparum*, in response to fosmidomycin. Our work demonstrates that fosmidomycin directly blocks de novo isoprenoid biosynthesis in both organisms. In addition, we provide the first confirmation that the biological effects of fosmidomycin are exclusively due to inhibition of isoprenoid metabolism, since fosmidomycin-mediated growth inhibition was rescued by media supplementation with a downstream isoprenol (geranylgeraniol). These studies provide important validation for antimicrobial and antimalarial drug development efforts that target the enzymes of non-mevalonate metabolism.

Our LC-MS/MS approach has confirmed the proposed two-step DXR reaction mechanism by detecting the putative reaction intermediate, 2-C-methylerythrose 4-phosphate, within both bacteria and malaria parasites. Previous enzymatic studies of DXR have monitored oxidation of its cofactor NADPH (which occurs during the second reaction step) and have therefore not distinguished whether fosmidomycin inhibits the first or second step in DXR catalysis (12, 27). The substantial accumulation of 2-C-methylerythrose-4-phosphate we observed following fosmidomycin treatment suggests that the second, reduction step of DXR (which converts 2-C-methylerythrose 4-phosphate to MEP) may be inhibited by fosmidomycin. Further analysis of the action of fosmidomycin on purified DXR is required to address this hypothesis.

The response of any given metabolic pathway to pharmacologic inhibition may be complex, since control mechanisms exist within biological systems to maintain homeostasis. In the absence of selective inhibitors of each of the non-mevalonate pathway enzymes, the relative contributions of these enzymes to flux through this pathway have not yet been quantified. With this in mind, we can conclude that the metabolic effects of fosmidomycin treatment are not consistent with a simple model in which fosmidomycin exclusively inhibits DXR, since the products of the DXR reaction did not decrease. Although DXR is an essential gene in *E. coli*, DXR null bacteria are viable when growth medium is supplemented with the alcohol form (ME) of the DXR product, MEP (3). In contrast, we found that ME did not completely rescue *E. coli* treated with fosmidomycin, even at high doses (1 mM), and did not restore growth in fosmidomycin-treated malaria parasites at all, indicating an additional, downstream target of fosmidomycin action within the isoprenoid biosynthesis pathway in these cells.

Metabolic profiling of fosmidomycin-treated *P. falciparum* and *E. coli* was most consistent with identification of IspD (2-C-methylerythritol-4-phosphate cytidyltransferase, EC 2.7.7.60) as the second target in both organisms—levels of all detected isoprenoid metabolites downstream of IspD fell, and isoprenoid metabolites upstream of IspD accumulated. Inhibition of purified IspD by fosmidomycin in vitro was weaker than expected, suggesting a more complicated model for the apparent IspD inhibition. The structure of *E. coli* IspD has been solved (31). We used Glide FX protein docking software (Schrödinger, Inc.) to model the interaction between IspD and either fosmidomycin or 2-C-methylerythrose 4-phosphate, the predicted DXR intermediate that accumulates in both fosmidomycin-treated bacteria and malaria parasites. While both small molecules dock preferentially into the CTP substrate-binding pocket of IspD, 2-C-methylerythrose 4-phosphate has an improved fit and forms five hydrogen bond contacts compared to two for fosmidomycin (Fig. S6). We speculate that IspD is inhibited by cellular 2-C-methylerythrose 4-phosphate that accumulates following fosmidomycin treatment or perhaps through other feedback control mechanisms within the cell.

Non-mevalonate isoprenoid biosynthesis is an essential biochemical pathway in eubacteria and in the malaria parasite *P. falciparum* and is not present in humans. These important attributes will continue to be exploited for development of novel antibacterial, antituberculous, and antimalarial agents. Our work will guide future medicinal chemistry efforts that depend on chemical modification of fosmidomycin. Our results also demonstrate a methodological advance that provides quantitative, non-radioactive detection of non-mevalonate isoprenoid precursors from less than 1 mL of bacterial culture, and that is suitable for evaluating organisms co-cultured with mammalian cells or harvested directly from humans.

Supplementary Material

Refer to Web version on PubMed Central for supplementary material.

Acknowledgments

We thank Dan Goldberg, Wes Van Voorhis, and Bill Hunter for generously providing reagents, and David Haslam for assistance with Glide FX. We thank Dan Goldberg, Alan Schwartz, and Phil Tarr for critical reviews and helpful suggestions.

References

1. Gershenzon J, Dudareva N. The function of terpene natural products in the natural world. Nat Chem Biol. 2007; 3:408–414. [PubMed: 17576428]

2. Hunter WN. The non-mevalonate pathway of isoprenoid precursor biosynthesis. J Biol Chem. 2007; 282:21573–21577. [PubMed: 17442674]
3. Kuzuyama T, Takahashi S, Seto H. Construction and characterization of *Escherichia coli* disruptants defective in the yaeM gene. Biosci Biotechnol Biochem. 1999; 63:776–778. [PubMed: 10361694]
4. Brown AC, Parish T. Dxr is essential in *Mycobacterium tuberculosis* and fosmidomycin resistance is due to a lack of uptake. BMC Microbiol. 2008; 8:78. [PubMed: 18489786]
5. Bryce J, Boschi-Pinto C, Shibuya K, Black RE. WHO estimates of the causes of death in children. Lancet. 2005; 365:1147–1152. [PubMed: 15794969]
6. Mayor S. WHO report shows progress in efforts to reduce malaria incidence. BMJ. 2008; 337:a1678. [PubMed: 18799523]
7. Fidock DA, Eastman RT, Ward SA, Meshnick SR. Recent highlights in antimalarial drug resistance and chemotherapy research. Trends Parasitol. 2008; 24:537–544. [PubMed: 18938106]
8. Dondorp AM, Nosten F, Yi P, Das D, Phyo AP, Tarning J, Lwin KM, Ariey F, Hanpithakpong W, Lee SJ, Ringwald P, Silamut K, Imwong M, Chotivanich K, Lim P, Herdman T, An SS, Yeung S, Singhasivanon P, Day NP, Lindegardh N, Socheat D, White NJ. Artemisinin resistance in *Plasmodium falciparum* malaria. N Engl J Med. 2009; 361:455–467. [PubMed: 19641202]
9. Cassera MB, Gozzo FC, D'Alexandri FL, Merino EF, del Portillo HA, Peres VJ, Almeida IC, Eberlin MN, Wunderlich G, Wiesner J, Jomaa H, Kimura EA, Katzin AM. The methylerythritol phosphate pathway is functionally active in all intraerythrocytic stages of *Plasmodium falciparum*. J Biol Chem. 2004; 279:51749–51759. [PubMed: 15452112]
10. Jomaa H, Wiesner J, Sanderbrand S, Altincicek B, Weidemeyer C, Hintz M, Turbachova I, Eberl M, Zeidler J, Lichtenthaler HK, Soldati D, Beck E. Inhibitors of the nonmevalonate pathway of isoprenoid biosynthesis as antimalarial drugs. Science. 1999; 285:1573–1576. [PubMed: 10477522]
11. Odom AR, Van Voorhis WC. Functional genetic analysis of the *Plasmodium falciparum* deoxyxylulose 5-phosphate reductoisomerase gene. Mol Biochem Parasitol. 2010; 170:108–111. [PubMed: 20018214]
12. Koppisch AT, Fox DT, Blagg BS, Poulter CD. *E. coli* MEP synthase: steady-state kinetic analysis and substrate binding. Biochemistry. 2002; 41:236–243. [PubMed: 11772021]
13. Sangari FJ, Perez-Gil J, Carretero-Paulet L, Garcia-Lobo JM, Rodriguez-Concepcion M. A new family of enzymes catalyzing the first committed step of the methylerythritol 4-phosphate (MEP) pathway for isoprenoid biosynthesis in bacteria. Proc Natl Acad Sci U S A. 2010; 107:14081–14086. [PubMed: 20660776]
14. Olliaro P, Wells TN. The global portfolio of new antimalarial medicines under development. Clin Pharmacol Ther. 2009; 85:584–595. [PubMed: 19404247]
15. Yu M, Kumar TR, Nkrumah LJ, Coppi A, Retzlaff S, Li CD, Kelly BJ, Moura PA, Lakshmanan V, Freundlich JS, Valderramos JC, Vilcheze C, Siedner M, Tsai JH, Falkard B, Sidhu AB, Purcell LA, Gratraud P, Kremer L, Waters AP, Schiehser G, Jacobus DP, Janse CJ, Ager A, Jacobs WR Jr. Sacchettini JC, Heussler V, Sinnis P, Fidock DA. The fatty acid biosynthesis enzyme FabI plays a key role in the development of liver-stage malarial parasites. Cell Host Microbe. 2008; 4:567–578. [PubMed: 19064257]
16. Cassera MB, Merino EF, Peres VJ, Kimura EA, Wunderlich G, Katzin AM. Effect of fosmidomycin on metabolic and transcript profiles of the methylerythritol phosphate pathway in *Plasmodium falciparum*. Mem Inst Oswaldo Cruz. 2007; 102:377–383. [PubMed: 17568945]
17. Dharia NV, Sidhu AB, Cassera MB, Westenberger SJ, Bopp SE, Eastman RT, Plouffe D, Batalov S, Park DJ, Volkman SK, Wirth DF, Zhou Y, Fidock DA, Winzeler EA. Use of high-density tiling microarrays to identify mutations globally and elucidate mechanisms of drug resistance in *Plasmodium falciparum*. Genome Biol. 2009; 10:R21. [PubMed: 19216790]
18. Giessmann D, Heidler P, Haemers T, Van Calenbergh S, Reichenberg A, Jomaa H, Weidemeyer C, Sanderbrand S, Wiesner J, Link A. Towards new antimalarial drugs: synthesis of non-hydrolyzable phosphate mimics as feed for a predictive QSAR study on 1-deoxy-D-xylulose-5-phosphate reductoisomerase inhibitors. Chem Biodivers. 2008; 5:643–656. [PubMed: 18421757]

19. Haemers T, Wiesner J, Giessmann D, Verbrugghen T, Hillaert U, Ortmann R, Jomaa H, Link A, Schlitzer M, Van Calenbergh S. Synthesis of beta- and gamma-oxa isosteres of fosmidomycin and FR900098 as antimalarial candidates. Bioorg Med Chem. 2008; 16:3361–3371. [PubMed: 18158249]
20. Wiesner J, Ortmann R, Jomaa H, Schlitzer M. Double ester prodrugs of FR900098 display enhanced in-vitro antimalarial activity. Arch Pharm (Weinheim). 2007; 340:667–669. [PubMed: 17994601]
21. Shigi Y. Inhibition of bacterial isoprenoid synthesis by fosmidomycin, a phosphonic acid-containing antibiotic. J Antimicrob Chemother. 1989; 24:131–145. [PubMed: 2676937]
22. Chen Q, Zhang B, Hicks LM, Wang S, Jez JM. A liquid chromatography-tandem mass spectrometry-based assay for indole-3-acetic acid-amido synthetase. Anal Biochem. 2009; 390:149–154. [PubMed: 19393612]
23. Luo B, Groenke K, Takors R, Wandrey C, Oldiges M. Simultaneous determination of multiple intracellular metabolites in glycolysis, pentose phosphate pathway and tricarboxylic acid cycle by liquid chromatography-mass spectrometry. J Chromatogr A. 2007; 1147:153–164. [PubMed: 17376459]
24. Trager W, Jensen JB. Human malaria parasites in continuous culture. Science. 1976; 193:673–675. [PubMed: 781840]
25. Corbett Y, Herrera L, Gonzalez J, Cubilla L, Capson TL, Coley PD, Kursar TA, Romero LI, Ortega-Barria E. A novel DNA-based microfluorimetric method to evaluate antimalarial drug activity. Am J Trop Med Hyg. 2004; 70:119–124. [PubMed: 14993620]
26. Hoeffler JF, Tritsch D, Grosdemange-Billiard C, Rohmer M. Isoprenoid biosynthesis via the methylerythritol phosphate pathway. Mechanistic investigations of the 1-deoxy-D-xylulose 5-phosphate reductoisomerase. Eur J Biochem. 2002; 269:4446–4457. [PubMed: 12230556]
27. Argyrou A, Blanchard JS. Kinetic and chemical mechanism of *Mycobacterium tuberculosis* 1-deoxy-D-xylulose-5-phosphate isomeroreductase. Biochemistry. 2004; 43:4375–4384. [PubMed: 15065882]
28. Bozdech Z, Llinas M, Pulliam BL, Wong ED, Zhu J, DeRisi JL. The transcriptome of the intraerythrocytic developmental cycle of *Plasmodium falciparum*. PLoS Biol. 2003; 1:E5. [PubMed: 12929205]
29. McFadden GI, Roos DS. Apicomplexan plastids as drug targets. Trends Microbiol. 1999; 7:328–333. [PubMed: 10431206]
30. Rohdich F, Lauw S, Kaiser J, Feicht R, Kohler P, Bacher A, Eisenreich W. Isoprenoid biosynthesis in plants - 2C-methyl-D-erythritol-4-phosphate synthase (IspC protein) of *Arabidopsis thaliana*. FEBS J. 2006; 273:4446–4458. [PubMed: 16972937]
31. Richard SB, Bowman ME, Kwiatkowski W, Kang I, Chow C, Lillo AM, Cane DE, Noel JP. Structure of 4-diphosphocytidyl-2-C-methylerythritol synthetase involved in mevalonate-independent isoprenoid biosynthesis. Nat Struct Biol. 2001; 8:641–648. [PubMed: 11427897]

Figure 1. Schematic of isoprenoid metabolism through the non-mevalonate pathway

The non-mevalonate pathway is the exclusive route to isoprenoid biosynthesis in eubacteria and the malaria parasite, *P. falciparum*. This pathway generates the basic isoprenoid building blocks IPP and DMAPP, which are elaborated to create diverse downstream products. Cell-permeable alcohol analogs of phosphorylated metabolites, such as ME (analog of MEP) and GG-ol (analog of GG-PP) are indicated by dotted arrows. Enzyme names in bold.

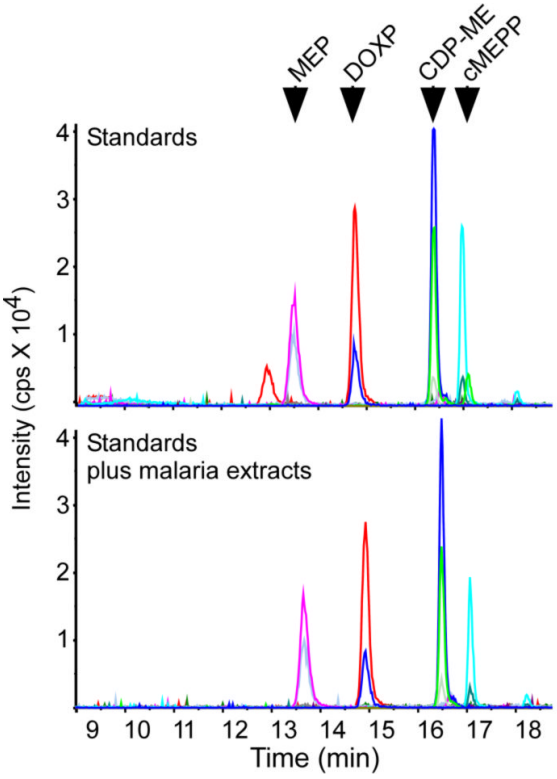

Figure 2. LC-MS/MS method detects metabolites of the non-mevalonate isoprenoid biosynthesis

Top, MRM traces of commercial standards of non-mevalonate isoprenoid precursors, demonstrating separation and detection of compounds of interest.

Bottom, MRM traces of equivalent commercial standards spiked with extracts from malaria parasites (that contain interfering metabolites), confirming that the separation method avoids signal quenching (ion suppression).

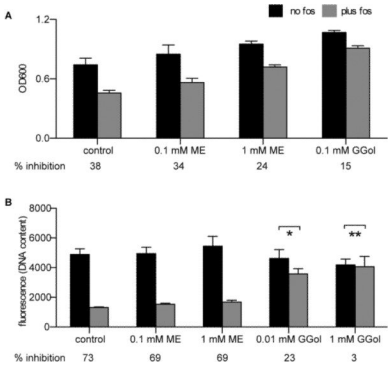

Figure 3. Geranylgeraniol rescues bacteria and malaria parasites treated with fosmidomycin

A, Growth of *E. coli* bacteria treated at logarithmic phase with (gray) and without (black) fosmidomycin and indicated compounds. Growth was monitored by OD_{600} at 10h. Mean and standard deviation values of three biological replicates are shown.

B, Growth of asynchronous blood-stage *P. falciparum* malaria parasites grown with (gray) and without (black) fosmidomycin and indicated compounds. Growth quantified by staining with the DNA fluorophore Picogreen (proportional to parasite number) following 3d of incubation. Mean and standard deviation values of three biological replicates are shown. *, p=0.222; **, p=0.763 (unpaired t-test comparing untreated and fosmidomycin-treated cultures).

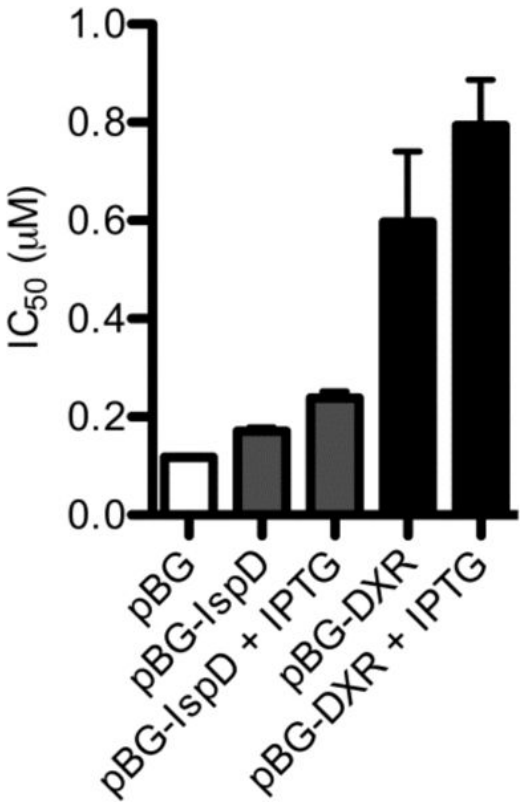

Figure 4. Overexpression of IspD confers fosmidomycin resistance

The half-maximal inhibitory concentration (IC_{50}) of fosmidomycin was determined for *E. coli* transformed with an empty vector (pBG), or either a vector expressing recombinant *E. coli* IspD protein (pBG-IspD) or *E. coli* DXR protein (pBG-DXR), with or without induction with IPTG. Values represent the mean and standard deviations of three independent experiments.

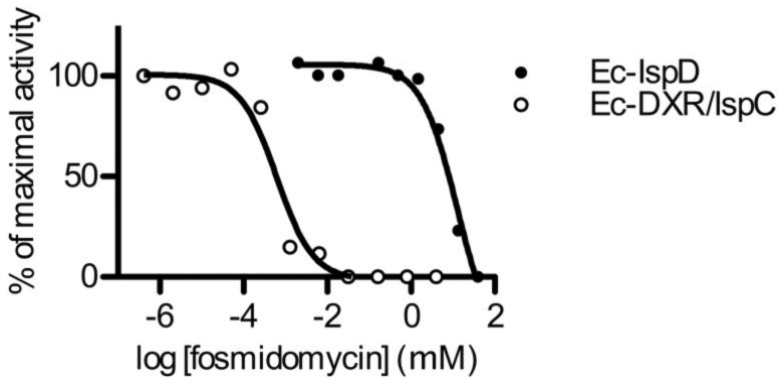

Figure 5. Fosmidomycin inhibition of IspD

Representative enzyme inhibition of recombinant *E. coli* IspD (Ec-IspD; closed circles) and *E. coli* DXR (Ec-DXR; open circles) proteins, assayed with increasing concentrations of fosmidomycin. The half-maximal inhibitory concentrations (IC_{50}) (from three independent replicates) are as follows: Ec-DXR, 0.81 +/− 0.27 μM; Ec-IspD 20.4 +/− 3.3 mM.

Table 1

Optimized parameters for multiple reaction monitoring (MRM) detection and quantification of targeted isoprenoid precursors[a]

Compound	Type of MRM	Q1 Mass (Da)	Q3 Mass (Da)	Dwell Time (ms)	DP	CE	CXP
DOXP	Qualifier	213	139	75	−42	−20	−4
	Quantifier	213	79	75	−42	−43	−4
	Qualifier	213	73	75	−42	−33	−4
Unknown 214 (methylerythrose-4-phosphate)	Qualifier	213	139	not present			
	Quantifier	213	79	75	−42	−43	−4
	Qualifier	213	73	75	−42	−33	−4
MEP	Qualifier	215	197	75	−48	−26	−4
	Qualifier	215	97	75	−48	−25	−4
	Quantifier	215	79	75	−48	−22.5	−4
CDP-ME	Quantifier	520	322	75	−80	−33	−2
	Qualifier	520	277	75	−80	−39	−2
	Qualifier	520	79	75	−80	−75	−2
CDP-MEP	Qualifier	600	520	50	−80	−18	−4
	Qualifier	600	384	50	−80	−50	−4
	Qualifier	600	277	50	−80	−30	−4
cMEPP	Qualifier	277	179	75	−54	−30	−7
	Qualifier	277	159	75	−54	−26	−7
	Quantifier	277	79	75	−54	−44	−7

[a]Entrance potential (EP) was set to 10V for all MRM transitions. Abbreviations: DP, declustering potential; CE, collision energy; CXP, collision cell exit potential. Voltage values are expressed in arbitrary units.

Table 2

Metabolic effects of fosmidomycin in *P. falciparum* malaria parasites[b]

compound (ag/cell)	t=0 (ring stage)	t=10h untreated	t=10h fosmidomycin treated	% of control values
DOXP	0.64 +/− 0.10	2.14 +/− 0.06	3.61 +/− 0.07	**169**
Unk 214	*	*	0.14 +/− 0.01	
MEP	*	*	0.51 +/− 0.10	**381**
CDP-ME	0.08 +/− 0.02	0.82 +/− 0.02	0.15 +/− 0.01	**18**
cMEPP	22.81 +/− 2.78	55.15 +/− 0.93	1.71 +/− 0.02	**3**

[b] LC-MS/MS quantification of isoprenoid precursors in ring stage *P. falciparum* parasites, in a single culture before (t=0) and after (t=10h) treatment with 5 μ*M* fosmidomycin. Treatment was begun early in blood-stage development and equivalent parasite numbers are present at t=10h. Fosmidomycin-treated samples are compared to untreated controls. Three independent biological replicates were performed, and the mean and standard error of the mean (SEM) values of three analytic replicates from a typical timecourse are shown. *, compound not detected. Lower limit of detection for the unknown 214 Da compound (Unk 214, presumptively identified as 2-C-methylerythrose 4-phosphate) is not known (no commercial standard available).

Table 3

Metabolic effects of fosmidomycin in *E. coli*[c]

compound (fg/cell)	t=0	t=1h	t=2h	t=4h	% of control values (at t=4h)
DOXP	0.145 +/− 0.004	4.191 +/− 0.049	2.738 +/− 0.030	3.107 +/− 0.125	**2,142**
Unk 214	*	0.135 +/− 0.001	0.070 +/− 0.003	0.147 +/− 0.009	
MEP	0.055 +/− 0.007	0.025 +/− 0.001	0.027 +/− 0.005	0.054 +/− 0.003	**98**
CDP-ME	0.092 +/− 0.010	*	*	*	**<10**
CDP-MEP	0.009 +/− 0.0005	*	*	*	
cMEPP	0.120 +/− 0.002	*	*	*	**<15**

[c]LC-MS/MS quantification of isoprenoid precursors in *E. coli* bacteria in a single culture during logarithmic growth, sampled at t= 0, 2, and 4h before and after fosmidomycin-treatment. Compound concentrations are normalized to bacterial cell number (1 OD_{600}= 10^9 cfu/mL). Compound concentrations at 4h after fosmidomycin treatment are compared to concentrations in the same culture prior to treatment. Three independent biological replicates were performed for each experiment, and the mean and SEM values of three analytic replicates from a typical timecourse are shown. *, compound not detected. Lower limits of detection for the unknown 214 Da compound (Unk 214, presumptively identified as 2-C-methylerythrose 4-phosphate) and CDP-ME are not known (no commercial standards available).

Biochemistry. Author manuscript; available in PMC 2012 May 3.